ELSEVIER

J. Non-Newtonian Fluid Mech., 68 (1997) 225–239

Journal of Non-Newtonian Fluid Mechanics

Analysis of dynamic mechanical data: inversion into a relaxation time spectrum and consistency check[1]

H. Henning Winter

Department of Chemical Engineering and Polymer Science and Engineering Department, Amherst, MA 01003–3110, USA

Received 25 November 1995; revised 5 July 1996

Abstract

This is an account of 8 years of experience with the same computer-aided methods (IRIS program; http://128.119.70.193/Lab/IRIS.html). The analysis of dynamical mechanical data consists of two main steps, conversion from the frequency to the time domain and check for consistency. Both are equally important. The first step is pretty much consolidated and some important progress can be reported with the second step which, however, has not received the attention deserved. The quality of the input data determines the limits of the calculated results. The analysis starts out with the postulate that there exists a continuous spectrum $H(\lambda)$ which then can be expressed in N discrete modes to express G', G'' data. The 'sampling frequency', N per decade, of the discrete representation cannot exceed a value of about 1.5–2 because of the noise in the data. To conclude the analysis, the discrete modes are converted into a continuous spectrum. The method of data analysis is outlined and characteristics of the solution are explored. © 1997 Elsevier Science B.V.

Keywords: Kramers–Kronig relation; Parsimonious model; Rheology; Relaxation time spectrum; Retardation time spectrum

1. Introduction

Macromolecules relax in a broad spectrum of relaxation times. The spectrum $H(\lambda)$ cannot be measured directly but it has to be extracted from stress/strain data of linear viscoelastic experiments. Major efforts have been undertaken worldwide for developing the best computer algorithm for that purpose [1–13]. While confidence in these algorithms has increased, nearly all the discussion has focused on the conversion methods themselves and not on the resulting spectra.

To appreciate the interest in the spectrum, it is important to realize that the time dependence of isochoric rheology is completely described by $H(\lambda)$, even at large strains or large strain rates (where an additional strain dependent perturbation of the equation is needed which is not

[1] Paper presented at the Polymer Melt Rheology Conference, University of Wales, Aberystwyth, 3–6 September 1995.

PII S0377-0257(96)01512-1

addressed here). The shape of $H(\lambda)$ is often correlated with specific molecular architectures. The spectrum's sensitivity to small changes in molecular connectivity makes it a powerful tool to distinguish small differences in otherwise indistinguishable materials. Systematic patterns have been found in $H(\lambda)$ which are useful for developing polymers of novel molecular architecture or for tailoring polymers to specific applications. Here it is especially important to avoid artefacts in the interpretation.

Mechanical spectrometry has grown into a mature field, mostly through advances in rheometer hardware combined with computer interfacing and data analysis. With ease, we can subject samples to well defined transient stresses and/or strains and not only measure the response but analyze it with interactive computer graphics. After that, we may simply use the data as obtained or we can ask further questions concerning data quality, completeness of the data set and limitations of applicability of the data. It is essential that these questions do not get neglected when the ease of data processing might give a false impression of safety. The result of such neglect could result in an over-interpretation of the data and a temptation to get drawn into conclusions which, upon closer inspection, are based on artefacts. More advanced methods have to be developed which not only convert data into some reduced parameter set but also show the inherent limitations of the result.

2. Experimental

Dynamic mechanical data contain all the information needed for calculation of the relaxation time spectrum, $H(\lambda)$. The storage modulus $G'(\omega)$ and the loss modulus $G''(\omega)$,

$$G'(\omega) = G_0 + \int_0^\infty H(\lambda) \frac{(\omega\lambda)^2}{1+(\omega\lambda)^2} \frac{d\lambda}{\lambda}, \tag{1}$$

$$G''(\omega) = \int_0^\infty H(\lambda) \frac{\omega\lambda}{1+(\omega\lambda)^2} \frac{d\lambda}{\lambda}, \tag{2}$$

are obtained from small amplitude oscillatory shear experiments over a sufficiently wide range of frequencies, $\omega_{min} \leq \omega \leq \omega_{max}$ (3 decades or more). Solids have an additional time-independent contribution, the equilibrium modulus G_0.

There are several important reasons for choosing G', G'' experiments over other linear viscoelastic experiments. These are:

(i) rapid development of quasi-steady state, in a time $\Delta t \approx 2\pi/\omega$;
(ii) selective probing of relaxation modes near $\lambda = 1/\omega$;
(iii) no zero drift problem of the transducer;
(iv) G' and G'' data contain same information (different weighting);
(v) the Kramers–Kronig relation allows a consistency check on G' and G'' data;
(vi) the limitation of a finite time window (truncation problem, see [14]).

Other linear viscoelastic experiments have served as a source for determining $H(\lambda)$, notably the relaxation modulus and the creep compliance. However, the information drawn from these material functions is often limited because of the problem of ill-posedness [15–17]. While it has not been possible to determine acceptable G' and G'' from $G(t)$ data, the opposite, determining

$G(t)$ from G', G'' data, is extremely accurate. With current rheometers, it might actually be more accurate to determine $G(t)$ from G', G'' data than to measure it directly in a step strain experiment.

The quality of the G', G'' data determines the outcome of the spectrum calculation. Three groups of effects have to be considered: truncation, systematic errors, and statistical errors (noise).

2.1. Truncation

The experimental frequency window, often extended by time–temperature superposition (performed with IRIS automatically or interactively on the computer screen), determines the relaxation time window, $1/\omega_{max} \leq \lambda \leq 1/\omega_{min}$, of the spectrum $H(\lambda)$ after completion of the data evaluation. Consequences of truncation have been studied by Jackson et al. [14], and they have been commented on quite frequently in the literature on modeling of viscoelastic liquid flow.

Each material (including solids) has a finite longest relaxation time λ_{max} which often is accessible by extending the experimental frequencies below $1/\lambda_{max}$. However, if this frequency is outside the experimental range, the long time tail will be missing from the calculated $H(\lambda)$. Attempts have been made to recover the long time tail by means of long time creep experiments. However, this does not really lead to satisfying results because of the above mentioned problem of ill-posedness in the data analysis.

A corresponding truncation occurs at the high frequency end of the G', G'' data. The only difference is that data are *always* truncated at the high frequency end since no lower limiting value exists for λ.

2.2. Systematic errors

Systematic errors are always present in the data but they are difficult to detect. An exception is the type of systematic error which leads to a violation of the Kramers–Kronig relation (see discussion below). Systematic errors might arise from various sources. Most typical are calibration errors of instrument settings and geometry. Often, they come from inconsistencies in the sample preparation, especially for polymers whose microstructures depend strongly on sample history.

2.3. Statistical errors

These can be seen when smoothing the data and evaluating the variance around the smooth curve. The proposed methods for $H(\lambda)$ calculation rely on data smoothing (filtering) in one way or another. Differences arise from the type of smoothing. Our proposal (the parsimonious model as discussed below) is to leave the data as they are and choose a fitting which is too coarse to reproduce the noise in the data. The degree of coarseness is determined by the noise in the data, i.e. it does not have to be predecided in the algorithm.

3. Desired properties of conversion algorithm

Each of the proposed methods in the literature has its strengths and weaknesses which should be evaluated in a critical comparison. This would go much beyond the scope of this report. However, we have tried to formulate basic criteria which an algorithm for determining $H(\lambda)$ should satisfy. The choice of these is an expression of personal preference rather than objective definition. Our preferences are the following.

1. Good fit of the experimental data.
2. Avoidance of overfitting. The algorithm should be able to find the optimum amount of detail which can be extracted from experimental data without producing artefacts.
3. The format of $H(\lambda)$ should not be predetermined. It has to be freely adjustable during the inversion of the data.
4. The resulting material parameters should have physical meaning.
5. Minimization of the truncation error. The data are always cut off on both sides of the frequency scale. This truncation may be the source of substantial error [14].
6. Checking of experimental data quality. The data are always inconsistent to some degree since the signal to noise ratios differs for G' and G''. This may cause a substantial discrepancy between fit and data which can be detected during data analysis.
7. For practical considerations, $H(\lambda)$ should be expressed by a function or a sum of functions which can be integrated easily in the various linear viscoelastic model calculations. This leads us to exponential functions for $H(\lambda)$.
8. For practical considerations, the number of parameters should be small (for ease of use in modeling calculations and for strong material data in a data bank).
9. For practical considerations, the computation time should be short. All conversion methods in the literature seem to satisfy this criterion, due to the high computation speed of desk top computers.

These criteria go much beyond the traditional search for an acceptable fit of the data in a reasonable time [18]. The algorithm is considered to be a basic tool for material characterization. The calculated spectrum is not seen as an end in itself but as starting information for rheological work. The applicability of the calculated spectrum and its consistency are prerequisites for a viable conversion method.

4. Method of evaluating $H(\lambda)$ from G', G'' data

To begin with, we assume that for our sample there exists a unique continuous function $H(\lambda)$ which describes its linear viscoelasticity. We further assume that $H(\lambda)$ is sufficiently smooth so that it can be taken as linear within small time intervals $[\lambda_i^-, \lambda_i^+]$ around λ_i. Our objective is to determine this function (or a close approximation of this function) in the best possible way according to the above criteria.

The computer algorithm for determining $H(\lambda)$ requires that we first discretize it. Since $H(\lambda)$ is mostly used in its integrated form, we proposed the following simple way of discretization [19]:

$$\int_0^\infty H(\lambda)\frac{\mathrm{d}\lambda}{\lambda} = \sum_{i=1}^{\infty}\int_{\lambda_i^+}^{\lambda_i^-} H(\lambda)\frac{\mathrm{d}\lambda}{\lambda} \approx \sum_{i=1}^{\infty} H(\lambda_i)\,\Delta_i, \tag{3}$$

with $\Delta_i = \ln(\lambda_i^- / \lambda_i^+) \approx \ln\sqrt{\lambda_{i-1}/\lambda_{i+1}}$. λ_i^- and λ_i^+ are the upper and lower time limits of the step Δ_i around λ_i. Note that Δ_i is positive since $\lambda_{i-1} > \lambda_{i+1}$ due to the convention of starting with the longest relaxation time, $\lambda_{\max} = \lambda_1$. As we will see below, Δ_i will be determined by the noise in the data. This is an important observation since our spectrum will not be able to detect $H(\lambda)$ variations which might occur at time scales smaller than Δ_i.

The continuous spectrum can be completely reconstructed from the discrete modes if the highest frequency in the wave representation of $H(\lambda)$ (Fourier series) is smaller than twice the 'discretizing frequency' [20]. This needs to be checked in each case, if possible. The discretizing frequency is defined as the reciprocal mode spacing $1/\Delta_i$. We will return to this criterion when choosing the density of the discrete relaxation modes.

For simplicity, the step size Δ_i could be chosen to be constant. In our calculations we treat Δ_i as a variable since this allows a closer fit of the data with fewer parameters. The discrete spectrum of Eq. (3) corresponds to a discrete relaxation modulus:

$$G(t) - G_0 \approx \sum_{i=1}^{\infty} H(\lambda_i)\,\Delta_i \exp(-t/\lambda_i). \tag{4}$$

Conventionally, this discrete relaxation is expressed as a sum of exponential decays (Maxwell modes).

$$G(t) - G_0 \approx \sum_{i=1}^{\infty} g_i \exp(-t/\lambda_i). \tag{5}$$

Thus, the values of H at the discrete times λ_i are connected to the front factors of this multimode viscoelastic material, g_i, by

$$g_i = H(\lambda_i)\,\Delta i. \tag{6}$$

To calculate one from the other, one needs to know the step size Δ_i which is provided from the solution set λ_i.

The data set extends over a finite time window, $1/\omega_{\max} \le t \le 1/\omega_{\min}$. Thus, only some finite number N is accessible from all the possible Maxwell modes. This specifies the parameter set which we plan to determine

$$g_i, \lambda_i \text{ with } i = 1, 2, 3, \ldots, N.$$

Both, g_i and λ_i are variable. The discrete spectrum expresses itself in discrete moduli:

$$G'(\omega) - G_0 = \sum_{i=1}^{N} g_i \frac{(\omega\lambda_i)^2}{1+(\omega\lambda_i)^2}, \tag{7}$$

$$G''(\omega) = \sum_{i=1}^{N} g_i \frac{\omega\lambda_i}{1+(\omega\lambda_i)^2}, \tag{8}$$

which can fit any G', G'' data with a suitable choice of parameters g_i, λ_i with $i = 1, 2, 3, \ldots, N$. The discretization does not introduce any loss of generality. Discrete spectrum and continuous spectrum are equivalent. It is important to realize that the discretization does not compromise the results in any way.

For an experiment with M data points, $[\omega_k, G'(\omega_k), G''(\omega_k)]$ with $k = 1, 2, 3, \ldots, M$, the deviation between fit, Eqs. (7) and (8), and data points may be expressed as a standard deviation S.D. with

$$\mathrm{SD}^2 = \frac{1}{M}\sum_{k=1}^{M}\left[1 - \frac{1}{G'(\omega_k)}\sum_{i=1}^{N}\frac{g_i(\omega_k\lambda_i)^2}{1+(\omega_k\lambda_i)^2}\right]^2 + \left[1 - \frac{1}{G''(\omega_k)}\sum_{i=1}^{N}\frac{g_i\omega_k\lambda_i}{1+(\omega_k\lambda_i)^2}\right]^2. \tag{9}$$

Minimization of S.D. (for constant N) results in a parameter set g_i, λ_i for the best fit. Our fitting program first places a large number of Maxwell modes, $g_{i,0}$, $\lambda_{i,0}$, evenly over the frequency range of the data, including an additional frequency decade on both sides. The modes can be calculated directly by solving a system of algebraic equations. A nonlinear fit follows in which g_i, λ_i and N are optimized to obtain the best fit of the data with a minimum number of modes.

The right choice of N is essential for the success of the algorithm. For small values of N, the spectrum is too coarse and model calculations with the spectrum appear wavy. The waviness and the deviation between fit and data decreases as we take more and more modes. This is documented in Fig. 1 where the minimized standard deviation S.D. (∂ S.D./$\partial g_i = \partial$ S.D./$\partial\lambda_i = 0$) decreases as N is allowed to grow. The noise in the data sets a natural limit to this improvement since the fit cannot be better than the standard deviation due to the noise. Taking more modes is not meaningful for two reasons: (a) the fitting does not improve significantly with these extra modes; (b) the values of all g_i start jumping erratically.

The S.D. curve basically consists of two arms, the steep one for improved fit of the sample parameters to G', G'' data, and the flat one for fitting the noise in the data. The crossover between these two regions is where we suggest to place N, i.e. the value of N depends on the noise level in the data. The resulting relaxation time spectrum has been termed the *parsimonious spectrum* [19] since it attempts the best fit with the fewest number of parameters.

The avoidance of over-fitting as described above is a well known process in control theory when modeling system behavior. Also, as we learned recently from Dr. Russell Davies, Aberystwyth, our findings are an example of the well established Morosov Discrepancy Principle [21] which expresses the fact that the fitting of data cannot be better than the S.D. in the data.

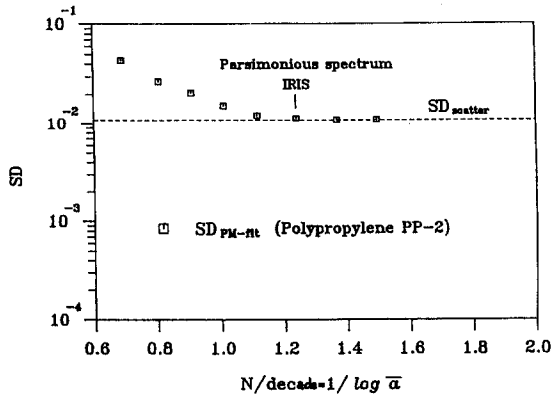

Fig. 1. The standard deviation between the best possible fit and data improves when the number of Maxwell modes, N, increases, Here the density of modes is defined as total number of modes divided by the number of decades in frequency of the experimental data input. The steep part of the curve describes the improved fitting of the real material behavior. The flat part of the curve describes the fitting of the noise in the data (from Ref. [19]).

Higher discretizing frequencies will reconstruct the high frequency variations (noise) in the data [20]. It would be possible to use higher discretizing frequencies and avoid noise reconstruction by introducing additional smoothing assumptions. These assumptions, however, can easily produce artefacts that are difficult to identify. We purposely avoid this phenomenon with the parsimonious modeling.

As the last step, the parsimonious spectrum needs to be converted back into the continuous spectrum with points $H(\lambda_i) = g_i/\Delta_i$ on the continuous line $H(\lambda)$.

The above result has been achieved without any manipulation of the data (such as smoothing) and it expresses the data with a minimum of parameters and within the S.D. of the data. It is extracting the information from the data to the fullest extent but it also avoids over-interpretation of the data which would lead to unacceptable artefacts.

5. Properties of the solution

Having completed the solution procedure, we are ready to explore the properties of the solution algorithm. This exploration is the most interesting part of the working on a computer algorithm since it most likely leads to unexpected results which call for explanation, as in a real experiment. We start out by searching for general trends in the behavior of the algorithm, then try to abstract these trends into general statements ('rules'), and check the limits at which they start to fail. Some of these properties will be discussed in the next paragraphs and often it will become clear that our observations need more rigorous proof before they will be acceptable in a more general context.

5.1. Ill-posedness

The inversion of a *single* integral equation such as Eq. (1) for G' (or Eq. (2) for G'') is known to be an ill-posed problem [15,17]. Little is known about the *simultaneous inversion of two interrelated integrals*. A surprising observation, contrary to statements in the literature, was that the typical characteristics of ill-posedness completely vanished when simultaneously performing the above inversion on both integrals for G' and G''. This lack of ill-posedness is most valuable for our purposes of finding the spectrum. Standard solution methods for ill-posed problems, such as Tikhonov regularization, are not needed here.

In analogy to the above observation, we can speculate that the *simultaneous* inversion of the relaxation modulus *and* the creep compliance might allow determination of the relaxation time spectra without encountering the problem of ill-posedness.

A frequently repeated statement, which might go back to Tanner [15], suggests that ill-posedness can be avoided with discrete relaxation spectra by keeping N small. Our algorithm also becomes more robust when reducing N. However, robustness does not seem to be our problem since the algorithm behaved in a well-posed way up to a high value of N as long as we worked with artificially smoothed data (smoothing for testing purposes only) ([19]). An upper limit occurred naturally at very high N at which the modes are so dense that rounding errors become important in the minimization procedure. The conclusion from our testing was that it is not any ill-posedness which creates an upper limit on N, but it is the noise in the data. This property has

been merely observed as an interesting and useful phenomenon, without trying to find any analytical proof.

5.2. Uniqueness

Several observations lead us to believe that the parsimonious spectrum poses a 'unique' solution to the problem (within experimental error). This is not obvious when only looking at the table of N discrete values g_i, λ_i and at variations in this table when changing the conditions of inversion. One needs to transform the discrete spectra g_i, λ_i into continuous form to see that, indeed, various very different looking discrete spectra reduce to the *same continuous function* $H(\lambda)$. In that sense, we call the discrete solutions unique since they are all equivalent representations of H. The various observations entail the following:

(i) the starting set $g_{i,0}, \lambda_{i,0}$ does not affect the final parsimonious spectrum;

(ii) random omission of several data points from the experimental input does not change the calculated continuous $H(\lambda)$;

(iii) addition of some artificial, random noise to the data does not affect the calculated continuous $H(\lambda)$ provided that we maintain about the same overall noise level.

In addition to these observations on real data, we produced artificial G', G'' 'data' from a known spectrum $H(\lambda)$. From these we calculated $H(\lambda)$, as described above, and always returned to the original spectrum [5,19]. This is an important test which needs to be satisfied by a conversion algorithm before considering it further.

The uniqueness of the parsimonious spectrum should be explored further, especially since most specialists in this field seem to claim non-uniqueness. It will be necessary to show uniqueness before further physical conclusions can be drawn from any experimental spectrum.

5.3. Weighting

The solution for the spectrum strongly depends on the weighting of the deviations in the definition of the S.D. We have used relative deviations, i.e. deviations between each experimental data point and its corresponding calculated data point divided by its absolute value. One can understand this as deviations on a logarithmic scale. This logarithmic scaling is necessary since the G', G'' values may vary over several decades. This had been recognized earlier [2] but does not seem to be generally known. Other weighting functions have been used in the literature but they cannot be recommended when analyzing data over a wide frequency window.

5.4. Negative g_i values

The possibility of negative g_i values for some of the modes of Eq. (5) has been considered in the literature ([22,23]). We have encountered such 'negtive modes' when modeling the noise in the G', G'' data. Smoothing of the data (for testing purposes) suppresses the occurrences of negative g_i values. We therefore assumed that negative g_i values were an artefact due to imperfection in the data. However, this working hypothesis needs to be substantiated further.

6. Computer aided consistency tests

The newly determined $H(\lambda)$ may be used in any of the linear viscoelastic material functions ([24]) and the result should be consistent with other experimental observations and with theory. The most obvious tests are:

plotting of G', G'' data against calculated G', G'' (from $H(\lambda)$);
plotting of deviations between the above functions vs. frequency;
plotting of relaxation modulus (from $H(\lambda)$);
plotting of creep compliance (from $H(\lambda)$);

All of these tasks are assigned to the computer (standard IRIS software) and the result is presented in interactive graphics mode. Specific tests are discussed in the following.

6.1. Kramers–Kronig relation

The storage modulus G' and the loss modulus G'' are not independent of each other. They are interrelated by the Kramers–Kronig relation;

$$\frac{G'(\omega)}{\omega^2} = \frac{2}{\pi}\int_0^\infty \frac{G''(x)}{\omega^2 - x^2}\frac{dx}{x}, \tag{10}$$

which has been described by Booij et al. [25] and by Bird et al. [26]. This relation is difficult to apply to experimental data since the low and high frequency tails extend beyond the data range. This is where discretization helps. The discrete form of Eq. (10)

$$\sum_{i=1}^{N} \frac{g_i\lambda_i^2}{1+(\omega\lambda_i)^2} = \frac{2}{\pi}\int_0^\infty \frac{1}{\omega^2 - x^2}\sum_{i=1}^{N}\frac{g_i\lambda_i}{1+(x\lambda_i)^2}\,dx \tag{11}$$

may be rearranged into

$$\sum_{i=1}^{N} g_i\lambda_i\left[\frac{\lambda_i}{1+(\omega\lambda_i)^2} - \frac{2}{\pi}\int_0^\infty \frac{1}{\omega^2 - x^2}\frac{1}{1+(x\lambda_i)^2}\,dx\right] = 0. \tag{12}$$

It can be shown by the function in the bracket is equal to zero for any λ_i. This means that each individual Maxwell mode g_i, λ_i satisfies the Kramers–Kronig relation. The equilibrium modulus G_0 is included in these calculations as a Maxwell mode with infinitely long relaxation time. The conclusion is that the discrete relaxation modulus, Eq. (5), will always satisfy the Kramers–Kronig relation.

This is a result which has far reaching implications for the evaluation of dynamic mechanical experiments. The spectrum calculation assessed in the above way tells us when a data set went wrong. If the computer algorithm is not able to fit a given set of G', G'' data, then this is reason to assume that the data set violates the Kramers–Kronig relation. Such violation can happen for various experimental reasons. We have used this criterion effectively for detecting faulty data sets. This is one of the greatest strengths of the parsimonious spectrum.

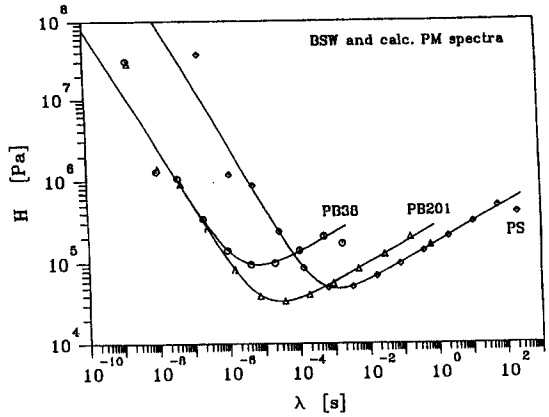

Fig. 2. Three BSW spectra (continuous lines), as in Baumgärtel et al. [32], have been used to calculate G', G'' values over a sufficiently wide frequency window. From these G', G'' values, we calculated spectra according to the parsimonious model (PM) method. The discrete points represent the solution. The input BSW spectrum has been recovered. Deviations arise from the sudden cut-off at λ_{max} and from truncation at short times. The BSW parameters were taken from Jackson et al. [28]. The discrete spectrum was calculated by M. Mours with the IRIS program.

6.2. Recovery of a known spectrum

The parsimonious spectrum has been calculated repeatedly for a wide range of different prescribed spectra, and the results were always consistent. Several of these tests have been published: 5-mode spectrum ([5]); 2-mode spectrum [5]; continuous spectra of three polypropylene melts ([19]); noisy spectrum ([19]). In another test, we prescribed a continuous spectrum of a polybutadiene melt [27],

$$H(\lambda) = mG_N^0\left[\left(\frac{\lambda}{\lambda_c}\right)^{-n} + \left(\frac{\lambda}{\lambda_{max}}\right)^{m}\right] \quad \text{for } \lambda \le \lambda_{max}, \tag{13}$$

calculated G' and G'' from that spectrum, and used them as a data set for testing the computer algorithm. The result shown as discrete points in Fig. 2 fits the prescribed spectrum very closely. Obviously, the sudden cut-off of the continuous spectrum can not be exactly reproduced with the discrete spectrum. This is a known property of discrete algorithms.

6.3. Prediction of other viscoelastic functions

Prediction based on the measured $H(\lambda)$ and comparison with experiment has to give consistent agreement. For instance, the limiting zero shear rate properties of viscosity and first normal stress coefficient are given by

$$\eta_0 = \int_0^{\lambda_{max}} H(\lambda)\,d\lambda \quad \text{and} \quad \psi_1 = 2\int_0^{\lambda_{max}} H(\lambda)\lambda\,d\lambda. \tag{14}$$

It is possible to model complicated transient experiments, as shown by Laun [2]. For example, in a *stress growth and relaxation* experiment a material is sheared initially with a constant strain rate, $\dot{\gamma}_0$, for a time t_0. The strain is then kept at a constant value. During this experiment the stress is recorded. In the linear viscoelastic region the stress response during the initial shear, $0 \le t \le t_0$, is given by

$$\tau(t) = \dot{\gamma}_0 \left[G_0 t + \sum_{i=1}^{N} g_i \lambda_i (1 - e^{-t/\lambda_i}) \right], \tag{15}$$

and first normal stress difference

$$N_1(t) = \dot{\gamma}_0^2 \left\{ G_0 t^2 + 2 \sum_{i=1}^{N} g_i \lambda_i^2 [1 - (1 + t/\lambda_i) e^{-t/\lambda_i}] \right\}, \tag{16}$$

and during stress relaxation ($t > t_0$)

$$\tau(t) = \dot{\gamma}_0 \left\{ G_0 t_0 + \sum_{i=1}^{N} g_i \lambda_i [e^{-(t-t_0)/\lambda_i} - e^{-t/\lambda_i}] \right\}, \tag{17}$$

$$N_1(t) = \dot{\gamma}_0^2 \left\{ G_0 t_0^2 + 2 \sum_{i=1}^{N} g_i \lambda_i^2 [1 - (1 + t_0/\lambda_i) e^{-t_0/\lambda_i}] e^{-(t-t_0)/\lambda_i} \right\}. \tag{18}$$

These predictions have been compared with experimental shear stress data of a liquid, a gel and a rubbery solid and the agreement was found to be acceptable [28].

A second very common experiment involves *creep and recovery*. Here the material is initially sheared under a constant stress, τ_0, for a time t_0 and the strain response is measured. In the linear viscoelastic region the strain response during initial shear, $0 \le t \le t_0$, is given by

$$\gamma(t) = \tau_0 \left(J_e + t/\eta_0 + \sum_{i=1}^{N-1} j_i (1 - e^{-t/\Lambda_i}) \right), \tag{19}$$

and during recovery ($t > t_0$)

$$\gamma(t) = \tau_0 \left\{ t_0/\eta_0 + \sum_{i=1}^{N-1} j_i [e^{-(t-t_0)/\Lambda_i} - e^{-t/\Lambda_i}] \right\}. \tag{20}$$

The retardation modes j_i, Λ_i, for $i = 1, 2, 3, \ldots, (N-1)$ can be determined from the relaxation spectrum [29]. These predictions agree well with experimental data [28].

Such modeling calculations are often useful for real applications. Instead of purchasing a creep rheometer one could, for instance, stay with the G', G'' measurement and calculate the creep behavior (the retardation spectrum for describing creep is fully determined by $H(\lambda)$ as shown by Gross [29]; see also Ref. [5]).

6.4. Onset of non-linearity

The relaxation time spectrum is also needed for calculating the stress at large strains. The most widely used model is that of Wagner [30] in which the stress is described by

$$\tau(t) = \int_{-\infty}^{t} \sum_{i=1}^{N} \frac{g_i}{\lambda_i} e^{-(t-t')/\lambda_i} h(t', t) C_t^{-1}(t') \, dt'. \tag{21}$$

Wagner's damping function h (I, II) depends on the invariants of the Finger strain tensor, $C_t^{-1}(t')$, between an instant t' in the past and the current time t. The invariants, I and II, are a measure of stretching of material lines and planes, respectively, between t' and t [31]. The onset of non-linearity is directly seen on the computer screen when plotting model calculations of start-up of shear or extension (from $H(\lambda)$) for comparison with experiment. The IRIS computer algorithm is designed for that purpose.

7. Conclusions

A robust procedure has been found for the calculation of relaxation time spectra $H(\lambda)$ from linear viscoelastic data G', G'', within the accuracy of the experiment. The same solution algorithm has been successfully used by us and others for 8 years. We prefer a most simple and transparent method of data analysis in order to avoid introduction of artefacts during the data conversion. The solution satisfies most of the chosen initial criteria.

(1) A close fitting of the data is very easy to achieve with a discrete function having narrow enough spacing between discrete relaxation modes. The fit of the data has always been close provided that the data satisfy the Kramers–Kronig relation.

(2) Over-fitting is avoided with the parsimonious model. We do not attempt a 'best fit', but a fit within the variance of the data. Other discrete spectra with a smaller standard deviation could be chosen. However, we do not accept this 'best fit' because of the artefacts which it would predict (violation of the Morozov discrepancy principle).

(3) All parameters in the set (g_i, λ_i, N) are freely adjustable during the minimization of S.D. The choice of Maxwell modes does not introduce any loss of generality and, hence, does not prescribe a specific form of the solution. Only if N is chosen to be too large (over-fitting) do assumptions have to be introduced about the solution. To avoid this, the average number of modes per decade, N per decade, should not exceed 1.5–2.

(4) The discrete values of g_i, λ_i of individual modes are not meaningful by themselves. They actually are replacable by other (g_i, λ_i, N) sets under different evaluation conditions. However, the continuous $H(\lambda)$ spectrum obtained from (g_i, λ_i, N) certainly is a meaningful representation of the macromolecular dynamics in a sample.

(5) The truncation error is relatively small because of the localized weight of exponential functions. However, it is still the most severe problem in the $H(\lambda)$ determination.

(6) The checking of data quality and limitations is an ongoing process. Several methods are available but more work is needed here. Interactive graphics combined with constitutive modeling help in this evaluation.

(7) The exponential functions are tractable in all the integrals which arise during any modeling.

(8) The number of parameters is naturally large for discrete representations. The parsimonious model searches for the minimum set within that framework.

(9) The spectrum calculation need only a few minutes on a conventional PC. The computation time increases with the width of the frequency window and is lower for higher quality data.

Good data over a sufficiently wide frequency window and at a high signal to noise ratio always give a meaningful $H(\lambda)$, i.e. the most severe limitations in the entire process arise from the actual measurement of G', G''.

Our current concerns are mostly with the evaluation of the solution and the estimation of its limits. The new generation of computer-aided methods in rheometry not only provides tools for analyzing but also attempts to evaluate the validity of experimental data. The very useful Kramers–Kronig check on the experimental data is an example. Another example is the parsimonious model which prevents over-fitting of the data. More work is needed in the estimation of the truncation error.

The mode density, N/decade, has to be chosen such that it satisfies the Morozov Discrepancy Principle and the Nyquist Theorem. The Morozov Discrepancy Principle gives an upper limit of N beyond which the data fitting becomes physically meaningless. We define this limit by the mode density at the transition from material fitting to noise fitting (marked as 'parsimonious spectrum' in Fig. 1). The Nyquist Theorem requires that this characteristic mode density (= discretizing frequency) is at least twice as high as the highest frequency in the wave representation of $H(\lambda)$. This normally is satisfied since (1) good experiments give reasonably high values for the characteristic mode density, and (2) the spectrum $H(\lambda)$ is a very gradually changing function (for most materials).

The general properties of the solution for $H(\lambda)$ are known, but they are still puzzling in many respects. The following features have been deduced from computer 'experimental' observations:

the crossover from material dominated to noise dominated fitting leads to the definition of the parsimonious spectrum:

the resolution of detail in the spectrum is given by the time step Δ_i which, in turn, depends on the quality of the experimental data; wave forms of $H(\lambda)$ with frequencies higher than $1/\Delta_i$ cannot be resolved;

the simultaneous inversion of two integrals suppresses the symptoms of ill-posed behavior;

the Kramers–Kronig relation allows a consistency check of data;

the solution $H(\lambda)$ is 'unique' (within experimental error and truncation error).

These factors should be analyzed further to come to a deeper understanding of why the solution works in the observed manner and where its limitations are.

Even with these unknowns, the parsimonious model has become a basic tool for the study of polymeric materials. One example is its application to G', G'' data of polystyrene standards which led to the finding of the universal spectrum for linear flexible polymers of uniform length [32]. The time has come for shifting the discussion away from the methods of determining $H(\lambda)$ and to the analysis of the spectrum itself.

Acknowledgements

The above ideas have developed during many discussions over years of collaboration with M. Baumgärtel, J. Jackson, M. DeRosa, F. Chambon, M. Mours, W. Wedler, P. Soskey and the other members of my research group. Much of this research was supported by General Electric and by the Materials Science and Engineering Center at the University of Massachusetts.

References

[1] K. Ninomiya, Effects of blending on the stress-relaxation behavior of polyvinyl acetate in the rubbery region, J. Colloid Sci., 14 (1959) 49.
[2] H.M. Laun, Description of the non-linear shear behavior of a low density polyethylene melts by means of an experimentally determined strain dependent memory function, Rheol. Acta, 17 (1978) 1.
[3] S.W. Provencher, A constrained regularization method for inverting data represented by linear algebraic or integral equations, Comput. Phys. Commun., 27 (1982) 213–227.
[4] S.W. Provencher, Contin: A general purpose constrained regularization program for inverting noisy linear algebraic and integral equations, Comput. Phys. Commun., 27 (1982) 229–242.
[5] M. Baumgärtel and H.H. Winter, Determination of the discrete relaxation and retardation time spectra from dynamic mechanical data, Rheol. Acta, 28 (1989) 511.
[6] V.M. Kamath and M.R. Mackley, The determination of polymer relaxation moduli and memory functions using integral transforms, J. Non-Newtonian Fluid Mech., 32 (1989) 119–144.
[7] J. Honkerkamp and J. Weese, Determination of the relaxation spectrum by a regularization method, Macromolecules, 22 (1989) 4372–4377.
[8] J. Honerkamp and J. Weese, Tikhonovs regularization method for ill-posed problems: A comparison of different methods for the determination of the regularization parameter, Continuum Mech. Thermodyn., 2 (1990) 17–30.
[9] J.C. Elster, J. Honerkamp and J. Weese, Using regularization methods for the determination of relaxation and retardation spectra of polymeric liquids, Rheol. Acta, 31 (1992) 161–174.
[10] N.W. Tschoegl and I. Emri, Generating line spectra from experimental responses. Part III. Interconversion between relaxation and retardation behavior, Int. J. Polym. Mater., 18 (1992) 117–127.
[11] N.W. Tschoegl and I. Emri, Generating line spectra from experimental responses. Part II. Storage and loss functions, Rheol. Acta, 32 (1993) 322–327.
[12] D.W. Mead, Numerical interconversion of linear viscoelastic material functions, J. Rheology 38 (1994) 1769–1795.
[13] C. Friedrich, H. Braun and J. Weese, Determination of relaxation time spectra by analytical inversion using a linear viscoelastic model with fractional derivatives, Polym. Eng. Sci., 35 (1995) 1661–1669.
[14] J.K. Jackson, C. Garcia-Franco and H.H. Winter, Modeling linear viscoelastic behavior with a truncated relaxation time spectrum, Ann. Tech. Meet. Soc. Plastics Eng. (ANTEC) 2438–2442, 1992.
[15] R.I. Tanner, Note on the iterative calculation of relaxation spectra, J. Appl. Polym. Sci., 12 (1968) 1649–1652.
[16] D.R. Wiff and M. Gehatia, Inferring mechanical relaxation spectra as an ill-posed problem, J. Appl. Phys., 46 (1975) 4231–4239.
[17] J. Honerkamp, Ill posed problems in rheology, Rheol. Acta, 28 (1989) 363–371.
[18] N. Orbey and J.M. Dealy, Determination of the relaxation spectrum from oscillatory shear data, J. Rheology, 35 (1991) 1035–1049.
[19] M. Baumgärtel and H.H. Winter, Interrelation between continuous and discrete relaxation time spectra, J. Non-Newtonian Fluid Mech., 44 (1992) 15–36.
[20] H. Nyquist, Certain topics in telegraph transmission theory, Trans Am. Inst. Elect. Eng., 47 (1928) 617–644.
[21] V.A. Morozov, Methods for Solving Incorrectly Posed Problems, Springer, Berlin, 1984.
[22] F. Akyildiz, R.S. Jones and K. Walters, On the spring-dashpot representation of linear viscoelastic behavior, Rheol. Acta, 29 (1990) 482–484.
[23] A.N. Beris and B.J. Edwards, On the admissibility criteria for linear viscoelasticity kernels, Rheol. Acta, 32 (1993) 505–510.
[24] J.D. Ferry, Viscoelastic Properties of Polymers, Wiley, New York, 1980.
[25] H.C. Booij and G.P.J.M. Thoone, Generalization of Kramers–Kronig transforms and some approximations of relations between viscoelastic quantities, Rheol. Acta, 21 (1982) 15–24.
[26] R.B. Bird, R.C. Armstrong and O. Hassager, Dynamics of Polymeric Liquids, Vol. 1, John Wiley & Sons, New York, 1987.
[27] J. Jackson, M. DeRosa and H.H. Winter, Molecular weight dependence of relaxation time spectra for the entanglement and flow behavior of monodisperse linear flexible polymers, Macromolecules, 27 (1994) 2426.

[28] H.H. Winter, M. Baumgärtel and S. Soskey, A parsimonious model for viscoelastic liquids and solids, in A.A. Collyer (Ed.), Techniques in Rheological Measurement, Chapman & Hall, London, 1993.
[29] B. Gross, Mathematical Structure of the Theories of Viscoelasticity, Hermann, Paris, 1953.
[30] M. Wagner, Analysis of time-dependent non-linear stress-growth data for shear and elongational flow of a low-density branched polyethylene melt, Rheol. Acta, 15 (1976) 136–142.
[31] H.H. Winter, On network models of molten polymers: loss of junctions due to stretching of material planes, Rheol. Acta, 17 (1978) 589–594.
[32] M. Baumgärtel, A. Schausberger and H.H. Winter, The relaxation of polymers with linear flexible chains of uniform length, Rheol. Acta, 29 (1990) 400–408.